Cell, Vol. 122, 887–900, September 23, 2005, Copyright ©2005 by Elsevier Inc. DOI 10.1016/j.cell.2005.06.044

Higher-Order Substrate Recognition of eIF2α by the RNA-Dependent Protein Kinase PKR

Arvin C. Dar,[1,2] Thomas E. Dever,[3] and Frank Sicheri[1,2,*]
[1]Program in Molecular Biology and Cancer
Samuel Lunenfeld Research Institute
Mount Sinai Hospital
600 University Avenue
Toronto, Ontario M5G 1X5
Canada
[2]Department of Molecular and Medical Genetics
University of Toronto
Toronto, Ontario M5S 1A8
Canada
[3]Laboratory of Gene Regulation and Development
National Institute of Child Health and Human Development
National Institutes of Health
Bethesda, Maryland, 20892

Summary

In response to binding viral double-stranded RNA byproducts within a cell, the RNA-dependent protein kinase PKR phosphorylates the α subunit of the translation initiation factor eIF2 on a regulatory site, Ser51. This triggers the general shutdown of protein synthesis and inhibition of viral propagation. To understand the basis for substrate recognition by and the regulation of PKR, we determined X-ray crystal structures of the catalytic domain of PKR in complex with eIF2α. The structures reveal that eIF2α binds to the C-terminal catalytic lobe while catalytic-domain dimerization is mediated by the N-terminal lobe. In addition to inducing a local unfolding of the Ser51 acceptor site in eIF2α, its mode of binding to PKR affords the Ser51 site full access to the catalytic cleft of PKR. The generality and implications of the structural mechanisms uncovered for PKR to the larger family of four human eIF2α protein kinases are discussed.

Introduction

The RNA-dependent protein kinase PKR belongs to a family that shares the ability to phosphorylate the α subunit of the translation initiation factor eIF2, a multisubunit G protein. Each family member, including PKR, the heme-regulated protein kinase HRI, the unfolded-protein-response regulator PERK, and the metabolite sensor GCN2, responds to distinct stress stimuli but transmits an overlapping signal that potently inhibits cellular translation through its ability to phosphorylate eIF2α on the same regulatory site, Ser51 (reviewed in Proud, 2005). The antiviral function of PKR is mediated by its ability to sense viral double-stranded RNA (dsRNA), a general byproduct of viral infection. The sensing of dsRNA by PKR and its downstream signaling response are facilitated by a domain architecture consisting of two dsRNA binding domains followed by a serine/threonine (Ser/Thr) protein kinase domain (Meurs et al., 1990). In binding dsRNA, PKR dimerizes and autophosphorylates on Thr446 within the activation segment of its catalytic domain. This leads to the full catalytic activation of PKR and the selective ability to phosphorylate eIF2α (Nanduri et al., 2000; Ung et al., 2001; Zhang et al., 2001). As a result of the phosphorylation of eIF2α on Ser51, eIF2 forms a high-affinity sequestering interaction with its own guanine nucleotide exchange factor, eIF2B. This complex inhibits the recycling of GTP for GDP on eIF2 prior to assembly of the 43S initiation complex, thus causing a general reduction in protein synthesis (reviewed in Dever, 2002).

Owing to its potent antiviral role, most viruses, including numerous human pathogens, have devised mechanisms to subvert PKR function. The growing list includes the oncogenic viruses hepatitis C and Epstein-Barr as well as herpes simplex virus, influenza virus, adenovirus, human immunodefiency virus, poliovirus, baculovirus, vaccinia virus, and reovirus (reviewed in Clemens, 2004). The study of the underlying mechanisms by which viruses subvert PKR function has shed light into the normal cellular workings of PKR. A case in point is the vaccinia virus protein K3L, which competitively blocks eIF2α phosphorylation by mimicking the three-dimensional structure of eIF2α and its mode of interaction with PKR (Kawagishi-Kobayashi et al., 1997; Sharp et al., 1997; Dar and Sicheri, 2002).

The precise mechanism by which PKR recognizes eIF2α and the mechanism by which dimerization and autophosphorylation control PKR catalytic activation and substrate recognition are long-standing areas of investigation. Oligomerization plays an essential role in regulating numerous protein kinases, most commonly through its ability to promote *trans*-autophosphorylation on regulatory sites both within and outside of the protein kinase catalytic domain (reviewed in Hubbard, 2004; Nolen et al., 2004; Dar et al., 2005). While dimerization could serve in part to promote *trans*-autophosphorylation of PKR by bringing two molecules in close proximity (Thomis and Samuel, 1995; Zhang et al., 2001), the observation that PKR dimerization is required for the recognition of eIF2α and for the sensitivity of PKR to the viral inhibitor protein K3L suggests that a specific dimer configuration may be an integral feature of PKR's active state (Dar and Sicheri, 2002).

PKR and the larger eIF2α protein kinase family employ a bipartite mechanism of substrate recognition. This is best illustrated by the fact that substitution of the Ser51 acceptor site in eIF2α for tyrosine still results in efficient phosphorylation by PKR (Lu et al., 1999) and that peptides derived from the Ser51 acceptor site of eIF2α are poor substrates as compared to the intact protein (0.6 μM versus 1080 μM, respectively; Mellor and Proud, 1991). A detailed understanding of the substrate-recognition determinants within eIF2α have been discerned by mutational analysis (Sharp et al., 1997; Dey et al., 2005a) together with the structure of the viral pseudosubstrate inhibitor K3L (Dar and Sicheri, 2002)

*Correspondence: sicheri@mshri.on.ca

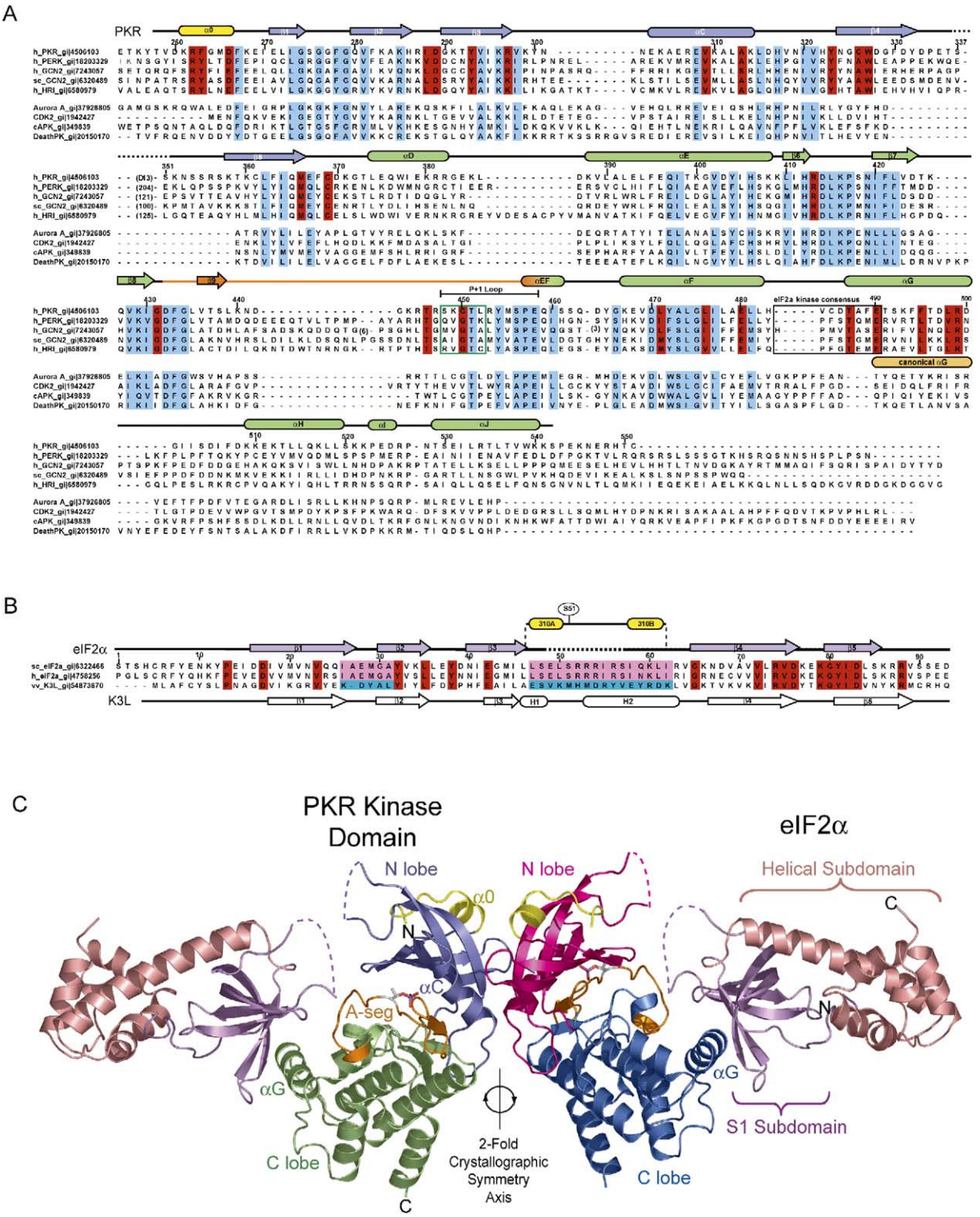

Figure 1. Structure of the PKR-eIF2α Complex

(A) Structure-based sequence alignment of the catalytic domains of human PKR, PERK, and HRI; human and *S. cerevisiae* GCN2; human Aurora A, cyclin-dependent, and death-associated protein kinases; and the mouse cyclic AMP-dependent kinase. Residues in blue are conserved across all protein kinases, while residues in red are conserved specifically amongst the eIF2α protein kinase family. Secondary-structure coloring scheme corresponds to that of the left PKR molecule shown in Figure 1C. Conservation of a noncanonical αF-αG linker and helix αG amongst the eIF2α protein kinases is denoted by a black box. The P+1 loop within the activation segment is denoted by a black line, and the distorted subelement (residues 448–452) is denoted by a green box. The orange cylinder denotes the canonical position and size of helix αG in non-eIF2α protein kinases.

and structures of eIF2α itself (Nonato et al., 2002; Dhaliwal and Hoffman, 2003; Ito et al., 2004). In brief, K3L and eIF2α employ a prestructured epitope to engage PKR that is presented by a common surface of their β barrel fold. The center of this prestructured epitope is remotely positioned 22 Å from the Ser51 phosphoacceptor site in eIF2α. In contrast, far less is known about the structural determinants for eIF2α recognition within PKR except that the determinants are fully contained within the catalytic domain and that recognition is dependent on catalytic-domain dimerization (Ung et al., 2001; Dar and Sicheri, 2002). In order to further our understanding of the molecular basis of eIF2α recognition by PKR and the structural role of dimerization and autophosphorylation in PKR function, we have determined X-ray crystal structures of the catalytic domain of PKR in complex with eIF2α.

Results

Structure Determination

A 284 amino acid fragment of human PKR and a 175 amino acid fragment of *S. cerevisiae* eIF2α were expressed separately in bacteria, purified to homogeneity, and mixed at a 1:1 molar ratio for crystallization. The PKR crystallization construct extends from residues 258 to 551 and encompasses the protein kinase catalytic domain. Two point mutations, His412Asn (Dar and Sicheri, 2002) and Cys551Ala, were engineered to reduce toxicity of PKR expression in bacteria by attenuating catalytic activity and to eliminate oxidation-induced protein instability, respectively. Additionally, a 13 residue deletion was introduced into the protease-sensitive β4–β5 loop of PKR (residues 338–350), which had the effect of eliminating the tendency of the protein to form high-molecular-weight aggregates at high concentrations, as evidenced by static light scattering. Importantly, the final crystallization construct forms a dimer in solution and maintains an ability to autophosphorylate on Thr446 and to phosphorylate eIF2α in vitro (Dey et al., 2005b [this issue of *Cell*]). The eIF2α fragment consists of the N-terminal two-thirds of the protein (residues 3 to 175 out of 303 total residues), which is similar to constructs analyzed previously by NMR and X-ray crystallography (Nonato et al., 2002; Dhaliwal and Hoffman, 2003; Ito et al., 2004). Crystals of a PKR/eIF2α complex diffracting to 2.8 Å (space group $P3_221$, a = b = 84.3 Å, c = 165.4 Å, α = β = 90°, γ = 120°) and a PKR/eIF2α complex bound to the ATP analog, β,γ-imidoadenosine-5′-triphosphate (AMP-PNP) and diffracting to 2.5 Å (space group $P2_1$, a = 64.7 Å, b = 48.8 Å, c = 133.4 Å, α = γ = 90°, β = 98.4°) were obtained. Structure determination of the $P3_221$ and $P2_1$ crystal forms were performed by molecular replacement (see Experimental Procedures) and refined to R_{factor}/R_{free} values of 20.7%/26.8% to 2.8 Å resolution and R_{factor}/R_{free} values of 22.8%/28.6% to 2.5 Å resolution, respectively. The asymmetric unit of the $P3_221$ crystal form consists of a single molecule each of PKR and eIF2α. The asymmetric unit of the $P2_1$ crystal form consists of two PKR molecules, two AMP-PNP molecules, and one eIF2α molecule. Data-collection and refinement statistics are listed in Table S1 in the Supplemental Data available with this article online. The final refined models display good geometry and Ramachandran statistics commensurate with the resolution of these studies. A representative composite simulated annealing omit electron density ($|2F_o - F_c|$) map centered on the phospho-Thr446 moiety of PKR is shown in Figure S1. Structure-based sequence alignments of the catalytic domains of the eIF2α protein kinases and the S1 subdomain of the eIF2α substrate and K3L pseudosubstrate proteins are shown in Figures 1A and 1B, respectively. A ribbon representation of the $P3_221$ crystal complex is shown in Figure 1C. A ribbon representation of the $P2_1$ crystal complex and detailed views of the individual PKR catalytic domains are provided in Figure S2. A detailed view of eIF2α and comparative views of previously determined isolated eIF2α and K3L structures are provided in Figure S3.

Overview of the PKR-eIF2α Complex and Individual Subunits

The catalytic domain of PKR adopts a bilobal structure typical of protein kinases, with a smaller N-terminal lobe (N lobe) and a larger C-terminal lobe (C lobe) connected by a short hinge (reviewed by Huse and Kuriyan, 2002). A higher-order dimeric configuration of the protein kinase domain is achieved by a back-to-back interaction of two N lobes, while the C lobe of PKR composes the binding site for eIF2α (Figure 1C). The dimer configuration of PKR is observed in both crystal forms analyzed. In the $P3_221$ crystal form, the dimer configuration is crystallographic in nature, while in the $P2_1$ crystal form, the same dimer configuration is generated by two distinct PKR molecules in the asymmetric unit. Identical binding modes of eIF2α to PKR are observed in both crystal forms; however, only one of two PKR molecules in the $P2_1$ crystal form engages an eIF2α molecule.

(B) Structure-based sequence alignment of the S1 subdomain of *S. cerevisiae* and human eIF2α and the vaccinia virus protein K3L. Secondary-structure elements of eIF2α complexed to PKR are colored magenta, while those of isolated K3L are colored white. Disorder of the helical insert of PKR bound eIF2α is represented by a dashed line, while secondary-structure elements of the corresponding region of isolated eIF2α are shown above in yellow. Residues that are invariant across the larger K3L/eIF2α protein family are colored red. Structurally divergent regions between K3L and eIF2α corresponding to the helix insert and the β1-β2 linker are colored blue and pink, respectively.

(C) Ribbons representation of the PKR/eIF2α complex ($P3_221$ crystal form) highlighting catalytic-domain dimerization mediated by the N lobe of PKR and eIF2α recognition mediated by the C lobe of PKR (see Figure S2 for $P2_1$ crystal form). The S1 subdomain (residues 3–90) and flanking helical subdomain (residues 91–175) of eIF2α are colored magenta and pink, respectively. The N and C lobes of PKR are colored purple and green (left molecule) and red and blue (right molecule), respectively. The activation segment (residues 432–458) and helix α0 (residues 260–266) of PKR are colored orange and yellow, respectively. The phospho-Thr446 side chain is shown in a ball-and-stick representation. Regions not modeled due to disorder and/or deletion in PKR (residues 338–351 corresponding to the eIF2α kinase characteristic insert) and eIF2α (residues 50–59 encompassing the Ser51 acceptor site) are shown as dashed lines.

PKR Subunit

The smaller N lobe of the kinase domain (residues 258–369) consists of a twisted five-strand antiparallel β sheet (denoted β1 to β5), a canonical helix αC laterally flanking one side of the β sheet, and a noncanonical helix α0 (residues 258–266), which integrates into the top groove of the β sheet. The β4–β5 connecting loop of PKR, corresponding to the site of deletion of an eIF2α kinase characteristic insert, is disordered. The larger C lobe (residues 370–551) is comprised of two paired antiparallel β strands (β7–β8 and β6–β9) and eight α helices (αD to αJ). Relative to protein kinase structures determined to date, only helix αG appears grossly displaced from a canonical position (C-terminal α helices αI and αJ are noncanonical elements). Positioned between helices αE and αEF in the lower catalytic lobe lies the activation segment (residues 432–458), which serves a phosphoregulatory function in many protein kinases, including PKR (reviewed in Johnson et al., 1996; Nolen et al., 2004). In the $P2_1$ crystal form, AMP-PNP binds at the cleft region of both PKR molecules, giving rise to a slightly more open configuration of catalytic lobes than is observed for PKR in the absence of bound nucleotide. The binding mode of AMP-PNP to PKR is generally the same as that observed in other active protein kinase structures (reviewed in Johnson et al., 1996; Nolen et al., 2004) (Figure 2A).

The activation segments of PKR in the $P3_221$ crystal form and of one PKR molecule in the $P2_1$ crystal form are stoichiometrically phosphorylated on Thr446 and adopt a fully structured winding conformation generally indicative of a catalytically competent state (Johnson et al., 1996; Nolen et al., 2004). This conformation is stabilized by the interaction of the Thr446 phosphate moiety with Lys304 and Arg307 side chains projecting from the N lobe helix αC and the Arg413 side chain projecting from the C lobe (Figure 2A). The Thr446 position and three phosphocoordinating residues are conserved in PKR, PERK, and HRI, but only Thr446 and Arg413 are conserved in GCN2 orthologs. In the second PKR molecule of the $P2_1$ crystal form, residues 437 to 451 of the activation segment are disordered (Figure S2C). Interestingly, this disorder correlates with disorder of the local eIF2α binding site of PKR, encompassing helix αG and also helix αD, and the absence of a bound eIF2α molecule (discussed below). The phosphorylation status of Thr446 in this molecule of PKR cannot be discerned.

A subelement of the activation segment, termed the P+1 loop, is notable for defining Ser/Thr versus tyrosine kinase specificity by providing a docking site for the phosphoacceptor sequence of the substrate in the immediate vicinity of the active site (reviewed in Nolen et al., 2004). A common inward position of the P+1 loop relative to the catalytic cleft is optimized for orienting shorter serine and threonine side chains to accept phosphate, while a common outwardly positioned loop is optimized for the longer tyrosine side chain (Figure 2B). The diagnostic presence of threonine at position 451 of the P+1 loop, versus the proline residue characteristic of tyrosine kinases, is consistent with the best-characterized function of PKR as a Ser/Thr-directed protein kinase (Figure 1A). However, PKR can also phosphorylate on tyrosine, although the biological relevance of this activity is not well understood (Lu et al., 1999). Interestingly, the conformation of the P+1 loop of PKR adopts an extreme outward orientation from residues 448 to 452, approaching that of a tyrosine kinase (Figure2B). Preceding and following this region, the activation segment of PKR returns to a canonical Ser/Thr protein kinase conformation. This unexpected outward orientation for part of the P+1 loop appears to be influenced by the absence of packing interactions with a noncanonically oriented helix αG and a direct hydrogen bond between the P+1 loop and the Glu28 side chain of eIF2α (Figures 2B and 3C). Since the phosphoacceptor sequence of eIF2α centered on Ser51 is not visible within the phosphoacceptor binding site of PKR (see below), the relevance of the P+1 loop distortion for orienting Ser51 for catalysis is unclear. However, if the P+1 loop distortion relates to the ability of PKR to phosphorylate on Ser/Thr and tyrosine residues (i.e., dual specificity), the P+1 loop distortion may have relevance for the mechanism of action of other dual-specificity protein kinases. Indeed, like PKR, most if not all dual-specificity protein kinases employ a P+1 loop signature motif diagnostic of Ser/Thr kinases and yet display the ability to phosphorylate on both Ser/Thr and tyrosine residues (Lindberg et al., 1992).

eIF2α Subunit

With the exception of the region surrounding the Ser51 phosphoacceptor site, the structure of eIF2α complexed to PKR is virtually identical to the X-ray crystal structure reported previously for an isolated *S. cerevisiae* protein fragment (Dhaliwal and Hoffman, 2003) and very similar to an X-ray crystal structure (Nonato et al., 2002) and solution structure (Ito et al., 2004) of human eIF2α. The eIF2α structure consists of an S1 subdomain (residues 3–90) flanked on one surface by a C-terminal α-helical subdomain (residues 91–175) (Figure S3). A major portion of the S1 subdomain, consisting of a five-strand β barrel (denoted β1 to β5), is highly conserved in primary and tertiary structure across the larger eIF2α and K3L protein family (Figure S3). The α-helical subdomain is unique to the eIF2α protein subfamily and consists of five α helices and one 3_{10} helix (denoted α1 to α5 and 3_{10}C). The S1 subdomain is interrupted on one surface of the β barrel, opposite to the site of association with the C-terminal α-helical subdomain, by a helical insert between β strands 3 and 4. The helical insert is notable for its structural conservation within but not across the eIF2α and K3L protein subfamilies (Dar and Sicheri, 2002). In the isolated *S. cerevisiae* and human eIF2α structures (Dhaliwal and Hoffman, 2003; Ito et al., 2004), the helical insert consists of two single-turn 3_{10} helices (denoted 3_{10}A and 3_{10}B) separated by a 7 residue linker containing the Ser51 phosphoregulatory site. High-atomic B factors for the helix insert of *S. cerevisiae* eIF2α (Dhaliwal and Hoffman, 2003) and a sensitivity of the helix insert of *S. cerevisiae* (F.S., unpublished results) and human eIF2α (Nonato et al., 2002) to proteolysis suggest a propensity for this region to undergo conformational change. The helix insert of K3L pseudosubstrates, in contrast, appears rigid and consists of a single-turn 3_{10} helix followed by a three-turn α helix (denoted helix 1 and 2, respectively) connected by a

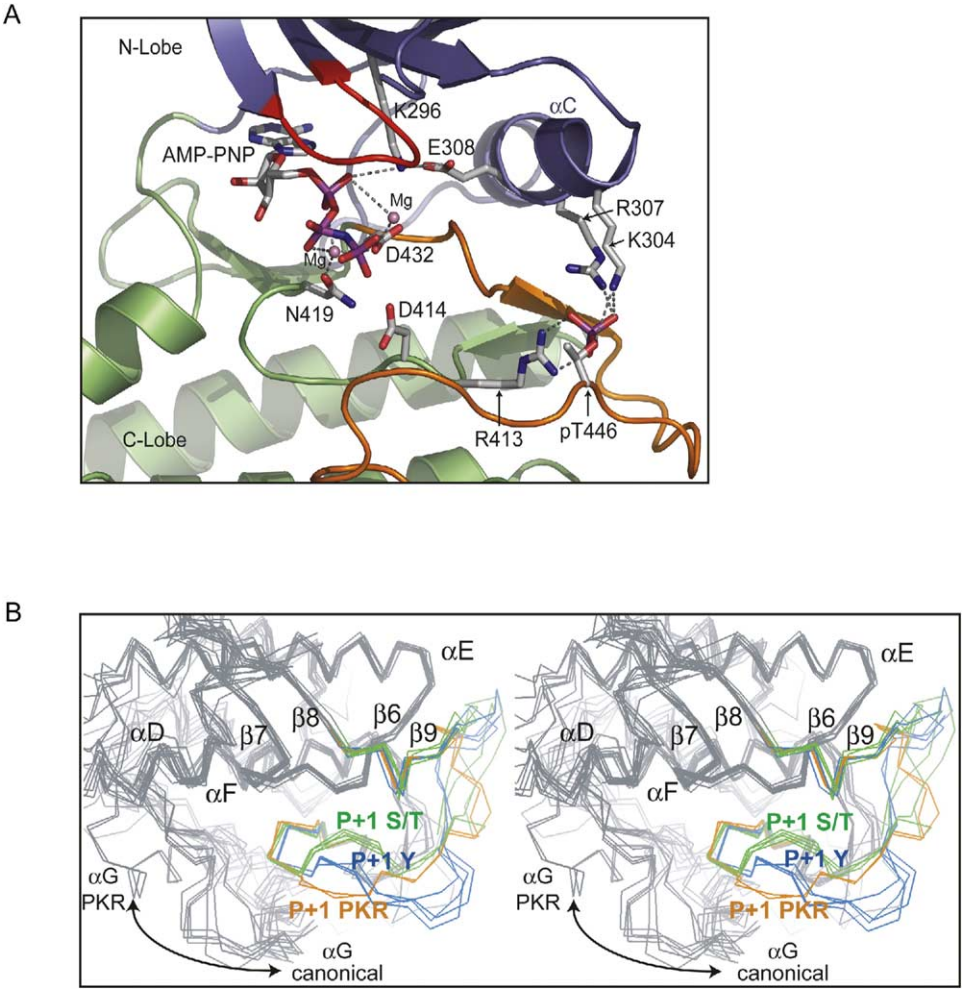

Figure 2. Active-Site Structure of PKR

(A) Frontal view of the catalytic cleft of PKR in complex with the ATP analog AMP-PNP ($P2_1$ crystal form, molecule #1). The coloring scheme follows that of Figure 1C (left molecule), with the G loop of PKR also colored red.

(B) Stereo view highlighting the P+1 loop of the activation segment of PKR and representative Ser/Thr and Tyrosine kinases in active states. Cα traces of activation segments are shown in color, while all other regions of the catalytic domains are shown in gray. The activation segments of two PKR molecules (from $P3_221$ and $P2_1$ crystal forms) are shown in orange; the tyrosine protein kinases IRK, IGFRK, c-KIT, and EGFRK are shown in blue (PDB ID codes 1IR3, 1K3A, 1PKG, and 1M14, respectively); and the Ser/Thr protein kinases PKA, PHK, CDK2, and ERK2 are shown in green (PDB ID codes 1JBP, 2PHK, 1H25, and 2ERK, respectively). A notable loss of packing interactions between the P+1 loop and the noncanonical position of helix αG in PKR, denoted by an arrow, may contribute to the forward orientation of the P+1 loop of PKR.

short 4 residue linker. As a possible consequence of binding to PKR, a majority of the helical insert of eIF2α, including the Ser51 phosphoregulatory site, is disordered (residues 49–56 and residues 49–60 in the $P2_1$ and $P3_221$ crystal forms, respectively).

The PKR/eIF2α Binding Interface

eIF2α engages the C lobe of the PKR catalytic domain at a region centered on the N-terminal end of helix αG. The total surface area buried by complex formation is ≈1200 Å^2 (1190 Å^2 and 1230 Å^2 in the $P3_221$ and $P2_1$ crystal forms, respectively). In binding PKR, eIF2α employs a surface of the β barrel involving all five β strands that is highly conserved across eIF2α and K3L proteins (Kawagishi-Kobayashi et al., 1997; Dar and Sicheri, 2002; Dey et al., 2005a). Indeed, projection of conserved residues onto the eIF2α surface almost perfectly identifies the contact surface with PKR (8 of 12 contact residues are highly conserved) (Figure 3A). Interestingly, on the reciprocal binding surface of PKR, only 2 of 13 contact residues are strongly conserved across the eIF2α protein kinase family, namely Thr487 and Glu490. In addition, many interactions involving eIF2α are directed at main-chain atoms of PKR. This apparent lack of conservation may account for the inability to locate the eIF2α binding site on PKR to date (Figure 3B, left panels).

eIF2α contacts two distinct elements of the C lobe of PKR through a diverse set of interactions including numerous water-bridged hydrogen bonds (Figure 3C). Most notable interactions are directed at helix αG, with the exception of hydrogen bonds directed at the activation segment of PKR. Interactions between eIF2α and PKR helix αG include (1) ionic and hydrophobic interac-

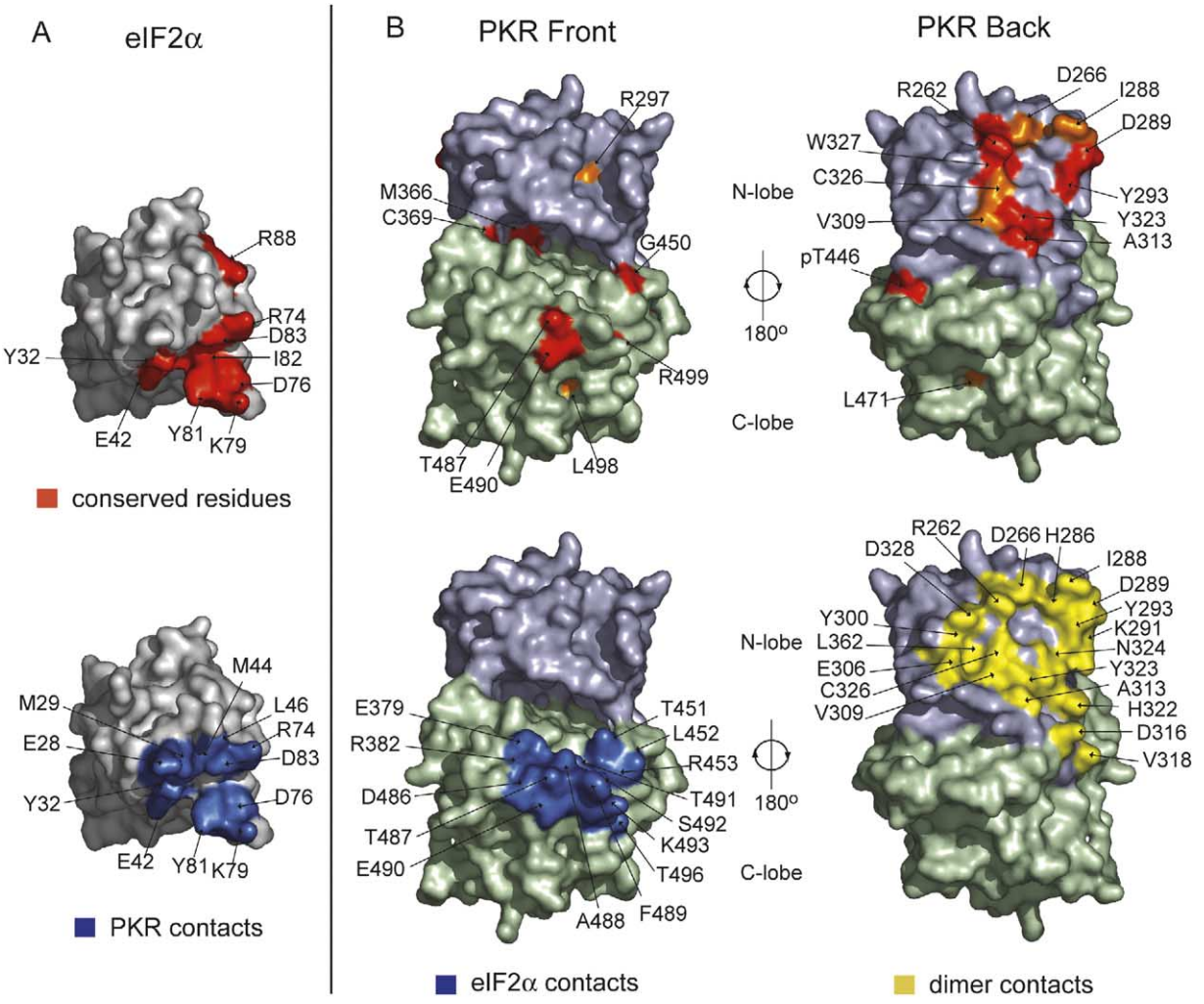

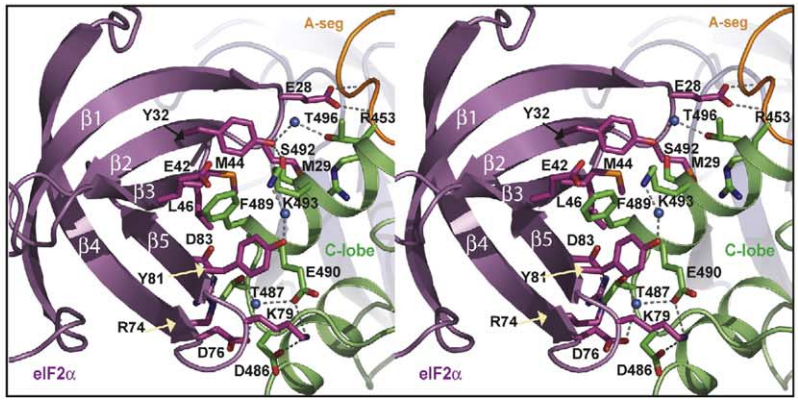

Figure 3. The PKR-eIF2α Complex

(A) Surface representation of eIF2α highlighting residues conserved across the larger K3L/eIF2α protein family in red (top panel) and residues that contact PKR in blue (bottom panel).

(B) Surface representations of front (left panels) and back (right panels) views of the catalytic domain of PKR. The N and C lobes of PKR are colored purple and green, respectively. Conserved residues across the eIF2α protein kinase family are colored red (top panels). Residues that contact eIF2α are colored blue (left bottom panel), while residues involved in catalytic-domain dimerization are colored yellow (right bottom panel).

(C) Stereo magnification of the binding interface between eIF2α and PKR. The S1 subdomain of eIF2α, shown in magenta, engages the C lobe of PKR, shown in green. Note that the activation-segment portion of the C lobe is shown in orange. Shown in ball-and-stick representation are residues that make notable interactions. For clarity, PKR contact residues Glu379, Ala488, Thr491, and Arg382 and the backbone amides of Thr451 and Leu452 (which hydrogen bond to Glu28 in eIF2α) have been omitted from this figure.

tions between the invariant Glu490 side chain of PKR and Lys79 and Tyr81 of eIF2α; (2) the side chain of Phe489 in PKR, which is substituted by either Met or Ser in other eIF2α kinases, projects into a hydrophobic pocket composed of Met44, Tyr32, Tyr81, and Glu42 side chains of eIF2α; and (3) the Asp83 side chain of eIF2α caps two of four backbone amino groups (Ala488 and Phe489) at the N terminus of PKR helix αG. In eIF2α protein kinases in which Phe489 is substituted for Ser (Figure 1A), our modeling studies suggest that a loss of hydrophobic interactions may be compensated for by a Ser side-chain hydrogen bond to Asp83 in eIF2α. Lastly, the invariant Thr487 residue of PKR makes few interactions of apparent consequence with eIF2α beyond van der Waals contacts to Arg74, Asp76, and Tyr81. Instead, Thr487 appears important for stabilizing helix αG by providing a third αG helix capping interaction to the backbone amino group of Glu490. Outside of helix αG, the backbone amide groups of Leu452 and Thr451 within the P+1 loop of the activation segment form optimal hydrogen bonds to the side chain of Glu28 in eIF2α (Figure 3C). As noted above, this interaction appears well placed to contribute to the nonstandard conformation of the P+1 loop in PKR.

A striking feature of the PKR/eIF2α binding mode centers on the unique size and the displaced position of helix αG in PKR. In a frontal comparison with other protein kinase structures, including PKR's closest structural homologs in the Protein Data Bank, Aurora A and the death-associated protein kinases (DAPK) (Figure 4A), helix αG of PKR is rotated counterclockwise 40° and translated 5 Å relative to its C terminus. This unique position of αG is attributable to the increased length of helix αG (one full turn longer) and the reduced length of the helix αF-αG linker (5 residues shorter) (Figures 1A and 4A). These two features combine to pull the N-terminal end of helix αG closer to helix αF. The overall effect of the noncanonical position and length of helix αG in PKR is twofold. First, the binding of eIF2α to helix αG optimally positions the helix insert of eIF2α toward the catalytic cleft of PKR. Although not visible in either crystal complex, the disordered Ser51 acceptor site of eIF2α can be modeled to engage the phosphoacceptor binding site of PKR without distortion to either PKR or eIF2α (Figure 4B). Second, the binding of eIF2α to helix αG occurs without physical clashes or distortion to other regions of PKR and eIF2α. In contrast, if helix αG of PKR were to adopt a canonical size and position, the Ser51 acceptor site of a bound eIF2α molecule would be too distant to access the phosphoacceptor binding site of PKR, and eIF2α would sterically clash with both N and C lobes of PKR (Figure 4C). These observations suggest that the noncanonical position of helix αG contributes to both eIF2α binding specificity and acceptor-site presentation to PKR.

Induced Conformational Change in the Phosphoacceptor Site of eIF2α

In order for PKR to phosphorylate eIF2α on Ser51, the helix insert of eIF2α must transition from the well-defined and -ordered state displayed in isolated structures (Dhaliwal and Hoffman, 2003; Ito et al., 2004) to the disordered state displayed by eIF2α in its PKR bound form. In the absence of a structural rearrangement, the Ser51 acceptor site would be positioned 17 Å away from the phosphoacceptor binding site in PKR (Figure 5A). In addition, in the isolated eIF2α structure, the Ser51 side chain appears inaccessible due to the structured environment of the helix insert (Figure 5B). This environment is maintained by a conserved local hydrophobic core involving the apolar side chains of Leu47, Leu50, Ile55, Ile58, Leu61, and Ile62 within the helical insert and Ile26 and Ala31 in the opposite-facing β1-β2 connecting segment. Demonstrating the protective nature of this local hydrophobic core, full-length eIF2α cannot be phosphorylated by the non-eIF2α protein kinase PKC to any detectable level, whereas short peptides derived from the Ser51 acceptor site are efficiently phosphorylated by PKC (K_M $eIF2\alpha^{residues\ 45–56}$ = 100 μM; Mellor and Proud, 1991).

As a result of binding to PKR, the main-chain position of the β1-β2 connecting segment and the C-terminal end of β strand 3 are physically shifted by 1.6 Å and 1.8 Å, respectively. While not large in absolute terms, these distortions appear significant relative to the absence of any changes to the eIF2α structure outside of the direct binding site. Excluding the disordered region and the main-chain elements in direct contact with PKR, the Cα atoms of free and bound eIF2α display a root-mean-square deviation (rmsd) of 0.57 Å, while ordered Cα atoms of main-chain elements in close contact with PKR display an rmsd of 2.4 Å (calculated on the $P2_1$ crystal form). Importantly, these conformational differences are maintained in both $P2_1$ and $P3_221$ crystal forms. Hence, together with the noted potential of the helix insert of eIF2α to undergo conformational change, binding to PKR appears to promote the unfolding of the helix insert of eIF2α to make the Ser51 site fully accessible to the phosphoacceptor binding site of PKR.

PKR Dimer Interface

In support of a structural role for dimerization in regulating PKR catalytic activity, the kinase domain of PKR adopts a well-defined dimer configuration in two different crystal environments (Figure 1C and Figure S2A). Furthermore, PKR dimer-interface residues are highly conserved across the eIF2α protein kinase family, suggesting general relevance of the dimer configuration for the functioning of all family members (Figure 3B, right panels and Figure 6). The PKR dimer interface is composed almost exclusively of N lobe elements, including helix α0, the β2-β3 connecting segment, a large portion of helix αC, and strands β4 and β5. The total surface area buried by dimer formation is 1370 $Å^2$ and 1760 $Å^2$ in the $P3_221$ and $P2_1$ crystal complexes, respectively. Due to small differences in the N lobe-to-N lobe contact angle imposed by crystal packing, not all dimer-interface contacts are equally represented in the $P3_221$ and $P2_1$ crystal structures (as noted below). Overall, the interaction surface is quite planar and involves a wide array of complementary hydrogen-bond, reciprocal salt, and hydrophobic interactions. Most notable amongst these include a hydrophobic interaction between the side chain of Ile288 at the tip of the β2-β3 linker and a hydrophobic pocket composed of Tyr300 in the β3-αC linker; Glu306, Val309, and Ala313 in helix αC; Cys326

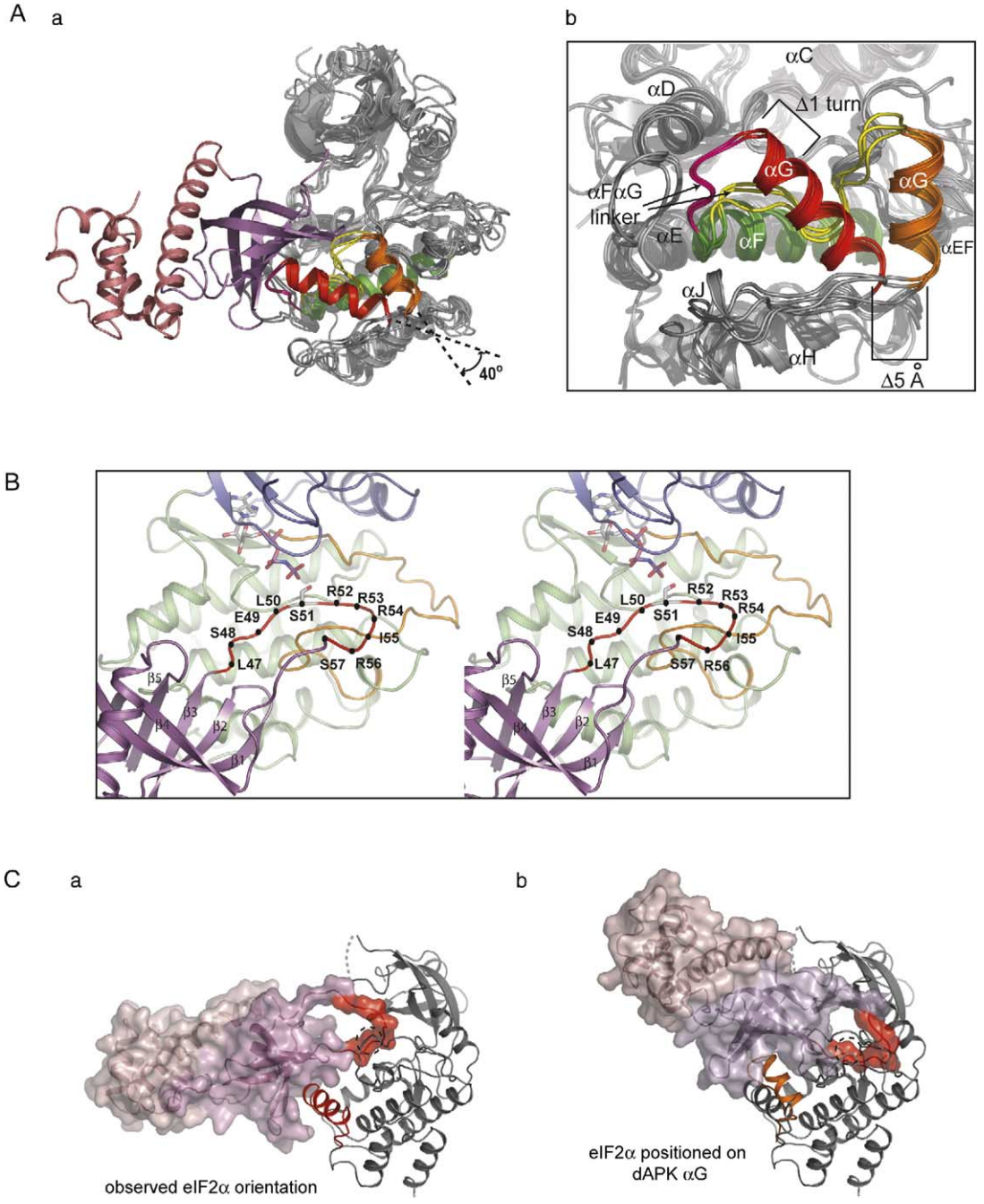

Figure 4. Basis for Selective Binding of eIF2α to PKR

(A) The eIF2α binding site on the catalytic domain of PKR is defined by a noncanonical orientation and size of helix αG. (Aa) Superposition of the catalytic-domain structures of PKR and its closest structural homologs, the death-associated protein kinase, Aurora A, and the cyclic AMP-dependent protein kinase (PDB ID codes 1IG1, 1MQ4, and 1JBP, respectively). Helix αF in each protein kinase is colored green. Helix αG of PKR is colored red, while those of the other protein kinases are colored orange. (Ab) Zoom-in view of helix αG detailing the shorter αF-αG linker and the increased length of helix αG in PKR.

(B) The disordered Ser51 acceptor site within the helix insert of eIF2α can be docked into the phosphoacceptor binding site of PKR without structural distortions to either protein. PKR and eIF2α are colored as in Figure 1C. The Ser51 acceptor site of eIF2α was modeled based on the structure of the phosphorylase kinase/peptide substrate complex (PDB ID code 2PHK; Lowe et al., 1997). The disordered region of the helix insert of eIF2α, shown in red, was modeled using Baton in O (Jones et al., 1991). Cα positions of the modeled helix-insert residues are labeled.

(C) Effect of helix αG position on eIF2α binding. (Ca) eIF2α binding to PKR helix αG in the noncanonical position observed in the $P3_221$ crystal structure. (Cb) Rigid-body reorientation of eIF2α to a canonical position of helix αG observed in the death-associated protein kinase (PDB ID code 1IG1). The disordered region in the eIF2α helix insert was modeled as in (B), with the Ser51 site circled.

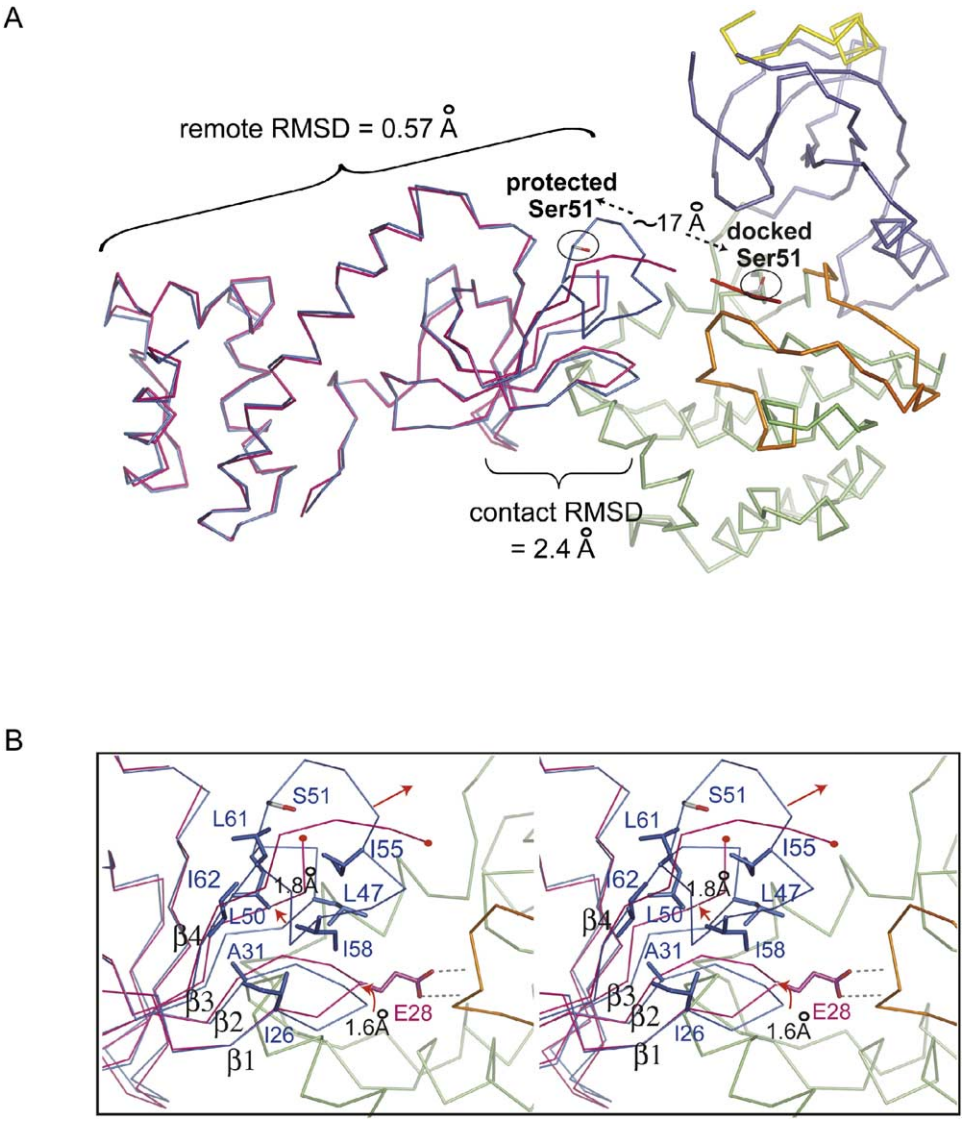

Figure 5. Conformational Change in eIF2α Induced by Binding to PKR

(A) Superposition of the eIF2α/PKR complex with the isolated *S. cerevisiae* eIF2α structure (PDB ID code 1Q46; Dhaliwal and Hoffman, 2003). Isolated eIF2α and eIF2α bound to PKR are shown in blue and red, respectively. The PKR catalytic domain is colored as in Figure 1C (left molecule). The two eIF2α structures were superimposed through a least-squares optimization of β strands 1–5 and α helices 1–5 (remote rmsd = 0.57 Å). All other regions of eIF2α display an rmsd (contact) variation of 2.4 Å. A phosphorylase kinase peptide substrate was docked to the phosphoacceptor binding site of PKR for comparison.

(B) Stereo magnification of the eIF2α/PKR contact site highlighting the local hydrophobic core that maintains order of the helix insert in the isolated *S. cerevisiae* eIF2α structure. Movements of secondary-structure elements in eIF2α resulting from contact with PKR, which may induce disorder in the helix-insert region of eIF2α, are demarked by arrows.

in strand β4; and Leu362 in strand β5 (Figure 6B). In addition, notable salt and hydrogen-bond interactions are observed between Arg262 and Asp266 in helices α0 (Figure 6) and between Asp289 and Tyr323. Hydrogen bonds are also observed (but not shown in Figure 6) between the side chain and the main-chain carbonyl of the two Asn324 residues (water-bridged in $P3_221$ crystal form), between the His286 side chain and the Cys326 backbone carbonyl (absent in $P3_221$ crystal form), and between the His322 side chain and backbone carbonyl of Tyr323 (absent in $P3_221$ crystal form).

While the visualized dimer configuration of PKR corresponds to the active state of the protein, a precise understanding of how dimerization directly impacts on catalytic activity must await the structure of the PKR catalytic domain in a repressed monomeric state. However, the provocative presence of helix αC, an active-site element underpinning the regulation of many protein kinases (reviewed in Huse and Kuriyan, 2002), within the dimer interface raises the possibility that helix αC could link dimerization to catalytic function.

Model for K3L Pseudosubstrate Binding to PKR

While the vaccinia virus protein K3L functions as a competitive inhibitor of eIF2α phosphorylation through its ability to engage a common higher-order binding

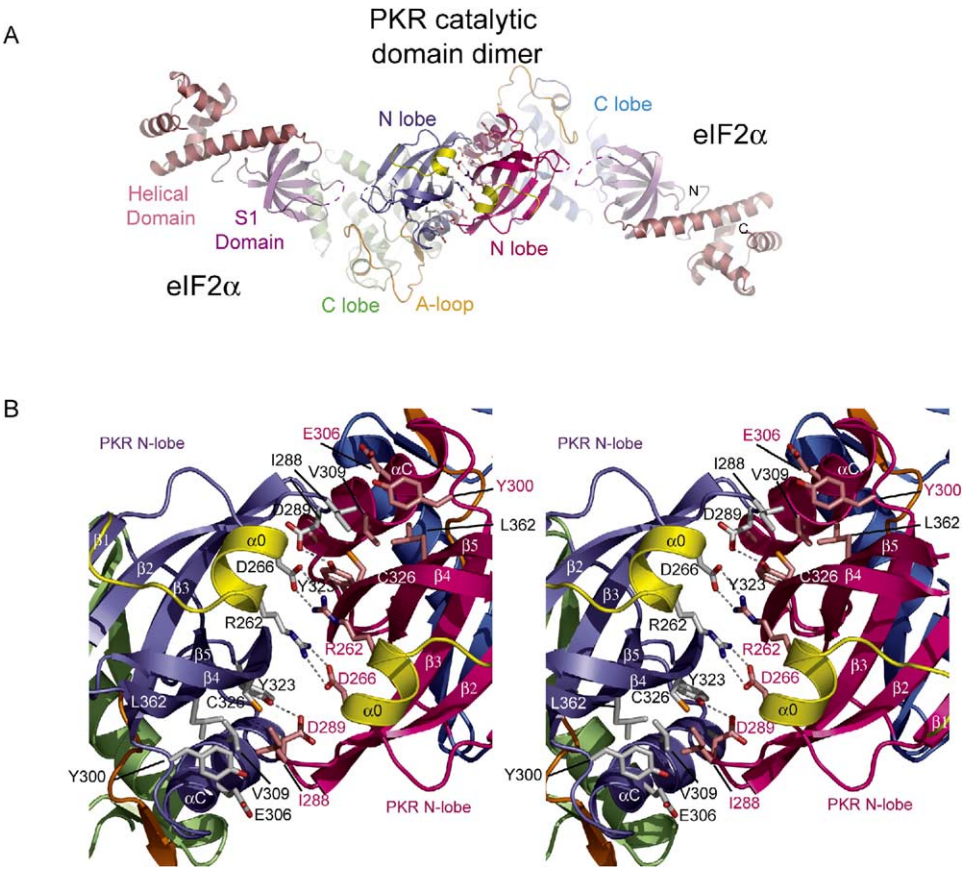

Figure 6. Ribbons Representation of the PKR/eIF2α Complex Highlighting the Catalytic-Domain Dimer Interface

(A) Perspective corresponds to a 90° rotation about the horizontal axis from Figure 1C. Ribbon elements are colored as in Figure 1C.

(B) Stereo magnification of the dimer interface as depicted in (A), with notable side chains displayed in ball-and-stick representation.

site on PKR (Kawagishi-Kobayashi et al., 1997; Sharp et al., 1997), K3L also functions as a noncompetitive and partial ($I_{max} \approx 78\%$) inhibitor of substrates that engage only the phosphoacceptor binding site of PKR (Dar and Sicheri, 2002). The latter function has been attributed to the unique conformation of the helix insert of K3L (Figure S3) and may provide the protein with a means to inhibit the activation of PKR by preventing *trans*-autophosphorylation or to subvert antiviral effects resulting from PKR phosphorylation of substrates other than eIF2α.

In order to gain insight into the basis for K3L's noncompetitive inhibitory function and the effect of previously characterized K3L mutations, we have generated a model of a K3L/PKR complex based on the eIF2α binding mode and a static structure of K3L (Figure 7A). Two novel features are apparent in the K3L/PKR complex that may be of relevance to K3L function. First, the most forward-projecting end of the helix insert, represented by the side chain of His47, is well positioned to interact with the activation segment of PKR without physically blocking the phosphoacceptor binding site. Suggesting that this may be a physiologically relevant contact, mutation of solvent-exposed His47 to Gln or Asp in K3L caused an average loss of approximately 20% in noncompetitive inhibitory efficiency without affecting overall binding to PKR (Dar and Sicheri, 2002). Meanwhile, substitution of Arg for His47 rendered K3L a more potent inhibitor of PKR in a yeast-based assay (Kawagishi-Kobayashi et al., 1997). Second, helix 1 and the β1-β2 linker of K3L form an extended contact surface with helix αG of PKR that is not observed in the eIF2α/PKR complex. Included on this surface is Val44 in helix 1, which, when mutated, markedly decreases binding affinity for PKR (Dar and Sicheri, 2002). Together, these data provide a framework for understanding how the divergent structure of the helix insert of K3L may impart functions not afforded through perfect mimicry of eIF2α.

Link between the Dimer Interface, the Activation Segment, and the eIF2α Binding Site

Previous binding studies and enzyme kinetic analyses demonstrated that, in addition to influencing catalytic function, PKR catalytic-domain dimerization also influences eIF2α and K3L recognition (Dar and Sicheri, 2002). In light of the crystal structures presented herein, the latter is difficult to rationalize since dimerization and substrate recognition occur on physically remote ends of the kinase domain. More recent experiments demonstrate that phosphorylation of the activation segment is absolutely essential for PKR substrate and pseudosub-

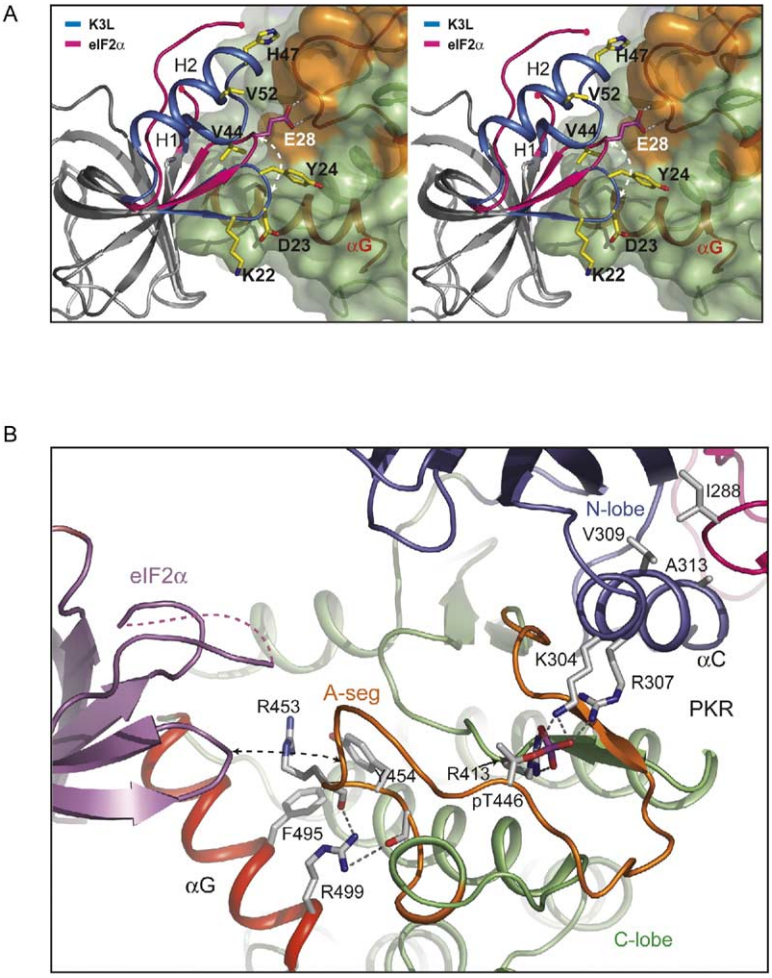

Figure 7. Models for K3L Binding and Allosteric Regulation of PKR

(A) Model of a PKR/K3L inhibitor complex based on the binding mode of eIF2α. Structurally distinct regions between K3L and eIF2α in the helical insert and β1-β2 linkers are colored blue and pink, respectively (See also Figure 1B). Regions of structural similarity between the K3L and eIF2α are colored gray. The semitransparent surface of PKR is colored green (C lobe) and orange (activation segment), with helix αG colored red. K3L residues, which have either been mapped by mutagenesis or lie in close proximity to helix αG in PKR, are highlighted in yellow. Glu28 of eIF2α, which contacts the activation segment of PKR, is colored pink.

(B) The activation segment of PKR provides a physical link between the catalytic-domain dimer interface and the eIF2α binding site. Conserved side chains contributing to a network of interactions that physically link helix αC to helix αG are shown in ball-and-stick representation. Ribbon elements are colored as in Figure 1C.

strate recognition (Dey et al., 2005b). In addition, these same studies demonstrate that activation-segment phosphorylation transitions the isolated kinase domain of PKR from a monomeric to a dimeric state (Dey et al., 2005b). Together, these data support the notion that the activation segment of PKR, which, as noted below, physically bridges the dimerization and substrate-recognition interfaces, serves to allosterically couple the two remote binding interfaces. In its phosphorylated state, the activation segment is stabilized in a productive conformation by phosphocoordinating interactions with conserved basic residues projecting from helix αC, while helix αC in turn composes an integral part of the dimer interface. Other regions of the activation segment make extensive (and likely conserved) contacts with helix αG, the principle binding site for eIF2α. Included are hydrogen-bond interactions between Arg499 at the base of helix αG and the backbone carbonyl groups of Arg453 and Met455 in the activation segment and a hydrophobic interaction between Tyr454 and Arg453 in the activation segment and Phe495 in helix αG (Figure 7B). Additionally, the activation segment of PKR also contacts eIF2α directly through a hydrogen-bond interaction involving Glu28 in the β1-β2 connecting segment and the backbone amide groups of Leu452 and Arg453 in the activation segment (represented by an arrow in Figure 7B). Further support for an allosteric coupling mechanism linking dimerization, activation-segment conformation, and substrate recognition is provided by one PKR molecule in the $P2_1$ crystal complex. In this molecule, the absence of an eIF2α binding partner correlates with local disorder of the eIF2α binding site on PKR and also disorder of the activation segment (Figure S2B versus Figure S2C). Since the phosphorylation status of Thr446 in this molecule cannot be assessed, the root cause of the observed disorder remains an open question. Indeed, the absence of an eIF2α binding partner imposed by crystal packing constraints (an eIF2α binding partner can not be accommodated in the crystal lattice) could alternatively be responsible for the observed disorder, and hence further structural studies of the repressed state of PKR will be required to fully resolve this issue.

Discussion

Similarities within the catalytic domains of the eIF2α protein kinase family suggest that the mechanisms of catalytic regulation and substrate recognition discerned from the PKR/eIF2α complex are functionally

relevant for the eIF2α protein kinase family as a whole. Indeed, as observed for PKR, dimerization and autophosphorylation appear to be an integral part of PERK, HRI, and GCN2 protein kinase function (Bertolotti et al., 2000; Bauer et al., 2001; Qiu et al., 2001). Demonstrating the potential relevance of an N lobe-to-N lobe mode of kinase-domain dimerization for PERK function, the eIF2α kinase invariant residue Arg587 in PERK (equivalent to Arg262 in PKR) is mutated in patients with a hereditary form of diabetes known as Wolcott-Rallison syndrome (Delepine et al., 2000). In the PKR structure, Arg262 forms a dimer contact with the invariant Asp266 residue, suggesting that a resultant defect in PERK dimerization may be the root cause of the disease pathology.

The role of dimerization in PKR catalytic activation differs critically from the classical activation paradigm of receptor tyrosine kinases (RTKs). As exemplified by the insulin and epithelial growth factor RTKs, ligand binding to the extracellular portion of the receptor promotes the juxtapositioning of intracellular catalytic domains to facilitate phosphorylation in *trans* by placing the activation segment of one kinase protomer into the active site of the other (reviewed in Hubbard, 2004). In the case of PKR, the back-to-back arrangement of the kinase-domain dimer precludes *trans*-autophosphorylation of molecules within a dimer since the activation segment of each protomer is inaccessible to the active site of the other. Therefore, PKR autophosphorylation must occur in *cis* or through the action of a PKR dimer on other PKR dimers or monomers. Further experiments are required to fully distinguish between these possible scenarios.

Based on conservation of the activation-segment phosphoregulatory site and basic phosphocoordinating residues, the importance of activation-segment phosphorylation for protein kinase regulation is likely fully conserved for three out of four human eIF2α kinases. For GCN2, the regulatory function of activation-segment phosphorylation may differ to some degree relative to PKR since GCN2 orthologs lack the equivalent of Arg307 and Lys304 residues in PKR projecting from helix αC that coordinate the Thr446 phosphate moiety. The presence of the third phosphate-coordinating residue in GCN2 is a general determinant of a functional dependence on activation-segment phosphorylation for protein kinases as a whole (Johnson et al., 1996). As GCN2 appears unique among eIF2α kinases in being a constitutive dimer (Qiu et al., 2001), perhaps this has negated a need to maintain the basic residues that couple dimerization status of the kinase domain to the conformation of the activation segment. The eIF2α recognition mechanism, in contrast, is fully conserved across the eIF2α protein kinase family, with the primary determinants appearing to consist of the unique size and orientation of helix αG rather than a strict conservation of residues composing the eIF2α contact surface. Sequence comparison reveals that all four members possess a short αF-αG helix linker and an atypically long helix αG (Figure 1A), and hence helix αG in each protein kinase likely adopts the noncanonical position observed for PKR.

Lastly, while PKR has been implicated in the regulation of numerous biological processes, no substrates other than eIF2α and PKR itself have been validated to date. Similarly, no additional substrates for PERK and HRI have been unambiguously identified despite a great divergence in their biological roles. In the case of GCN2, functional studies in *S. cerevisiae* are consistent with the existence of a single substrate for GCN2 and a single protein kinase for eIF2α phosphorylation on Ser51 (Dever et al., 1992). Although evolution has resulted in an increase from the single eIF2α protein kinase, GCN2, in *S. cerevisiae* to four eIF2α kinases in vertebrates, eukaryotic database searches reveal that only eIF2α possesses the "eIF2α/K3L"-like fold with the requisite amino acid determinants for binding PKR. This strongly suggests that the higher-order substrate-recognition mechanism employed by PKR and other eIF2α protein kinases, centered on helix αG, is restricted solely to eIF2α recognition. While these observations also hint at the possibility that the eIF2α protein kinase family, as a whole, phosphorylates only a single substrate, they do not rule out the possibility that PKR and other family members in vertebrates phosphorylate additional substrates through the use of alternate targeting mechanisms.

Experimental Procedures

Protein Expression and Purification

GST-PKR$^{258–551}$ and GST-eIF2α$^{3–175}$ were expressed separately in *E. coli* BL21 cells from TEV protease-cleavable versions of pET14b (Novagen) and pGEX-2T (Pharmacia) plasmids, respectively. Expressed proteins were bound to glutathione Sepharose and eluted by cleavage with TEV. Eluted PKR$^{258–551}$ and eIF2α$^{3–175}$ were applied to Q-Sepharose and Sp-Sepharose columns, respectively, and eluted with NaCl gradients, concentrated by ultrafiltration, and further purified by gel filtration chromatography (buffer = 10 mM HEPES, 150 mM NaCl, 5 mM dithiothreitol, 0.5 mM NaN_3 [pH 7.0] for PKR and PBS supplemented with 5 mM β-mercaptoethanol for eIF2α). Purified PKR$^{258–551}$ and eIF2α$^{3–175}$ were mixed at a 1:1 molar ratio to a final complex concentration of 0.5 mM (±2 mM AMP-PNP and 10 mM $MgCl_2$) for crystallization.

Crystallization, Data Collection, Structure Determination, and Modeling

Hanging drops containing 1 μl of complexes were mixed with equal volume of well buffer containing 10% (v/v) PEG 400, 100 mM $CaCl_2$, 0.1 M Tris (pH 8.0) for the $P3_221$ crystal form and 15% (v/v) PEG 400, 100 mM $CaCl_2$, 0.1 M Tris (pH 8.5) for the $P2_1$ crystal form. Crystals were cryoprotected with lower well solution supplemented with 30% (v/v) ethylene glycol prior to flash freezing in liquid N_2. Diffraction data for $P2_1$ and $P3_221$ crystal forms were collected at −170°C at APS beamline BM 14-C using an ADSC Q315 detector. Data processing and reduction was carried out with the HKL program suite (Otwinowski and Minor, 1997). The structure of the $P3_221$ crystal form was solved first by molecular replacement with CNS (Brunger et al., 1998) using eIF2α (PDB ID code 1Q46) and a PKR homology model based on the structure of PKA (PDB ID code 1ATP) as search models. Molecular-replacement solutions were modified and refined with alternate cycles of manual refitting and building into $|2F_o - F_c|$ and composite omit electron density maps using O (Jones et al., 1991) and simulated annealing and maximum likelihood protocols using CNS and REFMAC (Murshudov et al., 1997; Brunger et al., 1998). In the final model, residues 49–60 of eIF2α and residues 338–354 (corresponding to the site of our engineered loop deletion) and 542–551 (the C terminus) of PKR are disordered. Residues with disordered side chains modeled as Ala include Met29, Leu61, and Arg175 in eIF2α and Ser357 and Lys444 in PKR. Initial positions of a single eIF2α molecule and two PKR molecules in the $P2_1$ crystal form were identified by molecular replacement using the individual structures of eIF2α and PKR from

the $P3_221$ crystal form with the program PHASER (Storoni et al., 2004). The initial molecular-replacement solution was modified and refined as described for the $P3_221$ crystal form. In the final model, residues 49–56 of eIF2α and residues 334–355 and 542–551 of the directly bound PKR molecule are disordered. In the second PKR molecule, which lacked an eIF2α binding partner, significant portions of the C lobe were completely disordered, including residues 375–389 containing helix αD, residues 437–465 of the activation segment, and residues 483–500 of helix αG. As observed for molecule 1, residues 338–357 and 542–551 were also disordered. Residues with disordered side chains modeled as Ala include Gln59, Lys60, and Leu61 in eIF2α; Arg356, Lys426, Lys440, and Lys444 in PKR molecule 1; and Lys409, Lys416, Lys426, Tyr472, Lys509, Lys512, Gln516, Lys517, Leu518, Lys522, and Arg526 in PKR molecule 2. Pertinent refinement and data-collection statistics are listed in Table S1. Ribbons and surface representations were generated using PyMOL (DeLano, 2004). Superpositions for Figures 2B and 4A were generated using the program Swiss PDBViewer v3.7. The PKR kinase domain overlapped with IRK, IGFRK, c-KIT, EGFRK, PKA, PHK, CDK2, ERK2, DAPK, and Aurora A with rmsd values of 1.34 Å, 1.32 Å, 1.48 Å, 1.45 Å, 1.34 Å, 1.38 Å, 1.40 Å, 1.41 Å, 1.17 Å, and 1.26 Å, respectively. Superpositions of apo eIF2α, K3L, and bound eIF2α ($P2_1$ crystal form) were generated using a least-squares optimization with the program O (Jones et al., 1991).

Supplemental Data

Supplemental Data include one table and three figures and can be found with this article online at http://www.cell.com/cgi/content/full/122/6/887/DC1/.

Acknowledgments

We thank the BioCars staff at the Advanced Photon Source at Argonne National Laboratories, where diffraction data were collected. We thank Dan Durocher and Madhusudan Dey for helpful discussions during the preparation of this manuscript. We thank the members of the Sicheri laboratory for advice and for discussions. We thank Chune Cao for characterizing PKR cysteine mutants in a yeast-based assay and Alan Hinnebusch for SUI2 DNA. This work was supported in part by grants from the National Cancer Institute of Canada (F.S.) and by the Intramural Research Program of the NIH, NICHD (T.E.D.). A.C.D. is a recipient of a Canadian Graduate Scholarship from the Canadian Institutes for Health Research. F.S. is a recipient of a National Cancer Institute of Canada Scientist award.

Received: January 26, 2005
Revised: May 3, 2005
Accepted: June 28, 2005
Published: September 22, 2005

References

Bauer, B.N., Rafie-Kolpin, M., Lu, L., Han, A., and Chen, J.J. (2001). Multiple autophosphorylation is essential for the formation of the active and stable homodimer of heme-regulated eIF2alpha kinase. Biochemistry *40*, 11543–11551.

Bertolotti, A., Zhang, Y., Hendershot, L.M., Harding, H.P., and Ron, D. (2000). Dynamic interaction of BiP and ER stress transducers in the unfolded-protein response. Nat. Cell Biol. *2*, 326–332.

Brunger, A.T., Adams, P.D., Clore, G.M., Delano, W.L., Gros, P., Grosse-Kunstleve, R.W., Jiang, J.S., Kuszewski, J., Nilges, M., Pannu, N.S., et al. (1998). Crystallography and NMR system: A new software suite for macromolecular structure determination. Acta Crystallogr. *D54*, 905–921.

Clemens, M.J. (2004). Targets and mechanisms for the regulation of translation in malignant transformation. Oncogene *23*, 3180–3188.

Dar, A.C., and Sicheri, F. (2002). X-ray crystal structure and functional analysis of vaccinia virus K3L reveals molecular determinants for PKR subversion and substrate recognition. Mol. Cell *10*, 295–305.

Dar, A.C., Wybenga-Groot, L.E., and Sicheri, F. (2005). The eukaryotic protein kinase domain. In Modular Protein Domains, G. Cesareni, M. Gimona, M. Sudol, and M. Yaffe, eds. (Weinheim, Germany: Wiley-VCH Verlag GmbH & Co. KGaA), pp. 181–209.

DeLano, W.L. (2004). The PyMOL User's Manual (San Carlos, CA: Delano Scientific).

Delepine, M., Nicolino, M., Barrett, T., Golamaully, M., Lathrop, G.M., and Julier, C. (2000). EIF2AK3, encoding translation initiation factor 2-alpha kinase *3*, is mutated in patients with Wolcott-Rallison syndrome. Nat. Genet. *25*, 406–409.

Dever, T.E. (2002). Gene-specific regulation by general translation factors. Cell *108*, 545–556.

Dever, T.E., Feng, L., Wek, R.C., Cigan, A.M., Donahue, T.F., and Hinnebusch, A.G. (1992). Phosphorylation of initiation factor 2 alpha by protein kinase GCN2 mediates gene-specific translational control of GCN4 in yeast. Cell *68*, 585–596.

Dey, M., Trieselmann, B., Locke, E.G., Lu, J., Cao, C., Dar, A.C., Krishnamoorthy, T., Dong, J., Sicheri, F., and Dever, T.E. (2005a). PKR and GCN2 kinases and guanine nucleotide exchange factor eukaryotic translation initiation factor 2B (eIF2B) recognize overlapping surfaces on eIF2alpha. Mol. Cell. Biol. *25*, 3063–3075.

Dey, M., Cao, C., Dar, A.C., Tamura, T., Ozato, K., Sicheri, F., and Dever, T.E. (2005b). Mechanistic link between PKR dimerization, autophosphorylation, and eIF2a substrate recognition. Cell *122*, this issue, 901–913.

Dhaliwal, S., and Hoffman, D.W. (2003). The crystal structure of the N-terminal region of the alpha subunit of translation initiation factor 2 (eIF2alpha) from Saccharomyces cerevisiae provides a view of the loop containing serine *51*, the target of the eIF2alpha-specific kinases. J. Mol. Biol. *334*, 187–195.

Hubbard, S.R. (2004). Juxtamembrane autoinhibition in receptor tyrosine kinases. Nat. Rev. Mol. Cell Biol. *5*, 464–471.

Huse, M., and Kuriyan, J. (2002). The conformational plasticity of protein kinases. Cell *109*, 275–282.

Ito, T., Marintchev, A., and Wagner, G. (2004). Solution structure of human initiation factor eIF2alpha reveals homology to the elongation factor eEF1B. Structure (Camb.) *12*, 1693–1704.

Johnson, L.N., Noble, M.E., and Owen, D.J. (1996). Active and inactive protein kinases: structural basis for regulation. Cell *85*, 149–158.

Jones, T.A., Zou, J.Y., Cowan, S.W., and Kjeldgaard, M. (1991). Improved methods for binding protein models in electron density maps and the localization of errors in these models. Acta Crystallogr. *A47*, 110–119.

Kawagishi-Kobayashi, M., Silverman, J.B., Ung, T.L., and Dever, T.E. (1997). Regulation of the protein kinase PKR by the vaccinia virus pseudosubstrate inhibitor K3L is dependent on residues conserved between the K3L protein and the PKR substrate eIF2alpha. Mol. Cell. Biol. *17*, 4146–4158.

Lindberg, R.A., Quinn, A.M., and Hunter, T. (1992). Dual-specificity protein kinases: will any hydroxyl do? Trends Biochem. Sci. *17*, 114–119.

Lowe, E.D., Noble, M.E., Skamnaki, V.T., Oikonomakos, N.G., Owen, D.J., and Johnson, L.N. (1997). The crystal structure of a phosphorylase kinase peptide substrate complex: kinase substrate recognition. EMBO J. *16*, 6646–6658.

Lu, J., O'Hara, E.B., Trieselmann, B.A., Romano, P.R., and Dever, T.E. (1999). The interferon-induced double-stranded RNA-activated protein kinase PKR will phosphorylate serine, threonine, or tyrosine at residue 51 in eukaryotic initiation factor 2alpha. J. Biol. Chem. *274*, 32198–32203.

Mellor, H., and Proud, C.G. (1991). A synthetic peptide substrate for initiation factor-2 kinases. Biochem. Biophys. Res. Commun. *178*, 430–437.

Meurs, E., Chong, K., Galabru, J., Thomas, N.S., Kerr, I.M., Williams, B.R., and Hovanessian, A.G. (1990). Molecular cloning and characterization of the human double-stranded RNA-activated protein kinase induced by interferon. Cell *62*, 379–390.

Murshudov, G.N., Vagin, A.A., and Dodson, E.J. (1997). Refinement

of macromolecular structures by the maximum-likelihood method. Acta Crystallogr. D Biol. Crystallogr. *53*, 240–255.

Nanduri, S., Rahman, F., Williams, B.R., and Qin, J. (2000). A dynamically tuned double-stranded RNA binding mechanism for the activation of antiviral kinase PKR. EMBO J. *19*, 5567–5574.

Nolen, B., Taylor, S., and Ghosh, G. (2004). Regulation of protein kinases; controlling activity through activation segment conformation. Mol. Cell *15*, 661–675.

Nonato, M.C., Widom, J., and Clardy, J. (2002). Crystal structure of the N-terminal segment of human eukaryotic translation initiation factor 2alpha. J. Biol. Chem. *277*, 17057–17061. Published online February 21, 2002. 10.1074/jbc.M111804200.

Otwinowski, Z., and Minor, W. (1997). Processing of X-ray diffraction data collected in oscillation mode. Methods Enzymol. *276*, 307–326.

Proud, C.G. (2005). eIF2 and the control of cell physiology. Semin. Cell Dev. Biol. *16*, 3–12.

Qiu, H., Dong, J., Hu, C., Francklyn, C.S., and Hinnebusch, A.G. (2001). The tRNA-binding moiety in GCN2 contains a dimerization domain that interacts with the kinase domain and is required for tRNA binding and kinase activation. EMBO J. *20*, 1425–1438.

Sharp, T.V., Witzel, J.E., and Jagus, R. (1997). Homologous regions of the alpha subunit of eukaryotic translational initiation factor 2 (eIF2alpha) and the vaccinia virus K3L gene product interact with the same domain within the dsRNA-activated protein kinase (PKR). Eur. J. Biochem. *250*, 85–91.

Storoni, L.C., McCoy, A.J., and Reed, R.J. (2004). Likelihood-enhanced fast rotation functions. Acta Crystallogr. *D60*, 432–438.

Thomis, D.C., and Samuel, C.E. (1995). Mechanism of interferon action: characterization of the intermolecular autophosphorylation of PKR, the interferon-inducible, RNA-dependent protein kinase. J. Virol. *69*, 5195–5198.

Ung, T.L., Cao, C., Lu, J., Ozato, K., and Dever, T.E. (2001). Heterologous dimerization domains functionally substitute for the double-stranded RNA binding domains of the kinase PKR. EMBO J. *20*, 3728–3737.

Zhang, F., Romano, P.R., Nagamura-Inoue, T., Tian, B., Dever, T.E., Mathews, M.B., Ozato, K., and Hinnebusch, A.G. (2001). Binding of double-stranded RNA to protein kinase PKR is required for dimerization and promotes critical autophosphorylation events in the activation loop. J. Biol. Chem. *276*, 24946–24958.

Accession Numbers

The coordinates reported herein have been deposited in the Protein Data Bank with ID codes 2A1A and 2A19.